

## Soliton dynamics and interactions in dynamically photoinduced lattices

Ilias Tsopelas, Yannis Kominis, and Kyriakos Hizanidis

*School of Electrical and Computer Engineering, National Technical University of Athens, Zographou 15773, Greece*

(Received 30 May 2006; revised manuscript received 12 July 2006; published 15 September 2006)

The dynamics of a spatial soliton pulse and interactions under the presence of a linear periodic wave (PW), which dynamically induces a photonic lattice, is investigated. It is shown that appropriate selections of the characteristic parameters of the PW result in different soliton propagation and interaction scenarios, suggesting a reconfigurable soliton control mechanism. The quasiparticle perturbation method is utilized for providing a dynamical system, governing the soliton parameters evolution, for single- and two-soliton propagation under generic conditions for the PW. Results of the perturbation method are shown in good agreement with direct numerical simulations.

DOI: [10.1103/PhysRevE.74.036613](https://doi.org/10.1103/PhysRevE.74.036613)

PACS number(s): 42.65.Tg, 42.65.Sf

### I. INTRODUCTION

Light propagation in nonlinear photonic lattices and waveguide arrays is the subject of intense research interest in recent years, from both the theoretical and the experimental points of view [1,2]. The evolution of a soliton beam in a photonic lattice or a waveguide array has a rich set of interesting features that cannot be met in the case of homogeneous waveguides [3,4]. Such properties open a potential for practical technological applications related to photon management and control in terms of controllable soliton steering and switching [5–7]. Since the transverse structure of a nonlinear waveguide determines the soliton propagation characteristics, an appropriately designed periodic transverse pattern can efficiently control the beam evolution. However, this “static” control mechanism could be improved further, if the transverse structure of the waveguide is determined “dynamically” by a light source. Due to the intensity-dependent refractive index of a nonlinear waveguide, it is possible to use a control signal in order to modulate periodically the refractive index of the medium [8–13]. This approach has the benefit of dynamically reconfigurable control of soliton beams. On the other hand, the control signal can also be used for the dynamical modification of the interactions between solitons propagating in the same waveguide.

In this work, we study soliton dynamics and interactions under the presence of a linear dispersive periodic wave (PW), which dynamically modulates the nonlinear waveguide through the intensity-dependent refractive index. The underlying model of soliton propagation in a Kerr-type medium is the nonlinear Schrodinger (NLS) equation,

$$i\frac{\partial u}{\partial Z} + \frac{1}{2}\frac{\partial^2 u}{\partial X^2} + |u|^2 u = 0, \quad (1)$$

where  $X$  and  $Z$  are the transverse and the longitudinal dimensions normalized to the characteristic size of beam and to the diffraction distance, correspondingly, while  $u$  is the normalized beam amplitude.

We will show that even a small amplitude PW can significantly affect the soliton evolution, depending strongly on the relative parameters of both waves, and that appropriate choices of the parameter set of the control signal can result in

desirable soliton propagation characteristics. The quasiparticle perturbation method, employed in this work, extends the results of previous studies of single-soliton dynamics in photonic lattices by considering generic periodic profiles for the PW, instead of plane wave (purely sinusoidal) profiles [14,15], and also by taking into account the comparable length scales between the soliton width and the PW period [16–18]. The latter is of crucial importance, since as shown in Refs. [14,15], the case of comparable soliton width and PW period is particularly effective for soliton steering. The limiting cases of different length scales, corresponding to very narrow and wide beams, are included as special cases in our general approach. Moreover, the perturbation method is extended in order to study soliton interactions under the presence of the PW, resulting in a dynamical system describing the interplay between the mutual soliton interaction and the effect of the underlying PW. It is also shown that the evolution scenario of two initially well-separated solitons is strongly determined by the PW. The presence of the latter can either enhance or reduce the interaction between them. Results of the perturbation method for both single- and two-soliton dynamics under the presence of a PW, are compared. Good agreement with direct numerical simulations of Eq. (1) is demonstrated.

### II. SINGLE-SOLITON DYNAMICS

The NLS Eq. (1) has the well-known bright soliton solution

$$u_s(X, Z) = \eta \operatorname{sech}[\eta(X + \kappa Z - X_0)] \exp(-i\kappa X + i\sigma), \quad (2)$$

where  $\eta$  and  $\kappa$  are the beam amplitude and transverse velocity, respectively,  $X_0$  the initial beam center, and  $\sigma = 1/2(\eta^2 - \kappa^2)Z$ .

On the other hand, a low amplitude PW having the following Fourier expansion

$$u_{pw}(X, Z) = \sum_{n=-\infty}^{+\infty} a_n \exp[-i(k_n X + (1/2)k_n^2 Z + \phi_n)], \quad (3)$$

is a solution of the linear Schrodinger equation, where the nonlinear term is considered negligible. Following the same

approach as in Ref. [14], the superposition of the soliton and the PW is considered

$$u = u_s + u_{pw}. \quad (4)$$

Substitution of Eq. (4) in the NLS Eq. (1) results in a nonlinear term of the form

$$\begin{aligned} |u|^2 u = & |u_s|^2 u_s + u_s^2 u_{pw}^* + 2|u_s|^2 u_{pw} + 2u_s |u_{pw}|^2 + u_{pw}^2 u_s^* \\ & + |u_{pw}|^2 u_{pw}. \end{aligned} \quad (5)$$

By neglecting terms that are second and third order in  $u_{pw}$  we obtain the following perturbed NLS equation:

$$i \frac{\partial u_s}{\partial Z} + \frac{1}{2} \frac{\partial^2 u_s}{\partial X^2} + |u_s|^2 u_s = R(u_s, u_{pw}), \quad (6)$$

where

$$R(u_s, u_{pw}) = -(u_s^2 u_{pw}^* + 2|u_s|^2 u_{pw}) \quad (7)$$

is the perturbation term, which takes into account the modification of soliton propagation due to the presence of a PW. Applying a standard quasiparticle approach based on the perturbed-IST method [19,20], we obtain the following dynamical system governing the evolution of the soliton parameters, under propagation:

$$\frac{d\eta}{dZ} = \frac{\pi\eta^2}{2} \sum_{n=-\infty}^{+\infty} a_n \operatorname{sech}\left(\frac{\omega_n \pi}{2}\right) (\omega_n^2 + 1) \sin(A_n), \quad (8)$$

$$\frac{d\kappa}{dZ} = \frac{\pi\eta^2}{2} \sum_{n=-\infty}^{+\infty} a_n \omega_n \operatorname{sech}\left(\frac{\omega_n \pi}{2}\right) (\omega_n^2 + 1) \sin(A_n), \quad (9)$$

$$\begin{aligned} \frac{dX_0}{dZ} = & -\kappa - \frac{\pi}{2} \sum_{n=-\infty}^{+\infty} a_n \operatorname{sech}\left(\frac{\omega_n \pi}{2}\right) \\ & \times \left[ -\frac{\pi}{2} \tanh\left(\frac{\omega_n \pi}{2}\right) (\omega_n^2 + 1) + 2\omega_n \right] \cos(A_n), \end{aligned} \quad (10)$$

$$\begin{aligned} \frac{d\sigma}{dZ} = & \frac{1}{2} (\eta^2 - \kappa^2) + X_0 \frac{d\kappa}{dZ} + \frac{\pi\eta}{2} \sum_{n=-\infty}^{+\infty} a_n \operatorname{sech}\left(\frac{\omega_n \pi}{2}\right) \\ & \times \left[ \frac{\omega_n \pi}{2} \tanh\left(\frac{\omega_n \pi}{2}\right) (\omega_n^2 + 1) + 2 \right] \cos(A_n), \end{aligned} \quad (11)$$

where  $\omega_n = (k_n - \kappa) / \eta$  and  $A_n = (k_n - \kappa) X_0 + (1/2) k_n^2 Z + \sigma - \phi_n$ . Equations (8)–(11) define a nonautonomous system of two degrees of freedom. It explicitly describes the effect of each spectral component of the PW on the soliton evolution dy-

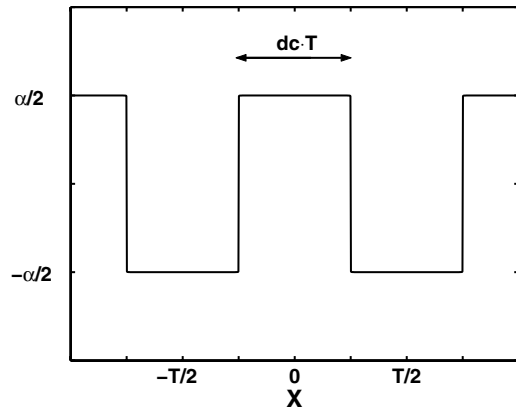


FIG. 1. Periodic wave with a rectangular amplitude profile of amplitude  $a$ , period  $T$ , and duty cycle  $dc$ .

namics. At this point it must be emphasized that the system has been derived under no assumption on the length scales of the soliton width and the PW period. As a result, the equations describing soliton width and velocity evolution are coupled, in contrast to the cases where the soliton width differs significantly as compared to the PW period [16–18]. The latter cases result in a much simpler one-degree-of-freedom autonomous dynamical system. They, however, exclude the applicability of the results to comparable length scales, where complex dynamics are expected to occur due to resonances between the longitudinal wave number of the soliton  $[(1/2)\eta^2]$  and the wave numbers of the PW Fourier components  $[(1/2)k_n^2]$ . Although the dynamical system (8)–(11) applies for any kind of PW, for illustrative purposes, we consider in the following, a PW having a rectangular amplitude profile (shown in Fig. 1) and a transverse velocity  $k$ .

For the case of zero transverse velocity  $k=0$ , the PW carries no momentum and its effect on soliton propagation results in steadily breathing solitons undergoing amplitude (width) and chirp oscillations [21], while for large PW periods (with respect to soliton width), soliton “swinging” with zero average transverse velocity has been shown to occur [16]. More interesting (from the point of view of potential applications to reconfigurable soliton control), is the case  $k \neq 0$  on which we are focusing in the rest of this work. In this case the PW can transfer momentum to the soliton leading to controllable drift and steering of the latter [14,15]. Considering (without loss of generality) a zero initial soliton transverse velocity  $\kappa=0$ , the presence of the PW results in soliton dragging by the dynamically evolving PW-induced lattice. In the following, a soliton of unitary amplitude  $\eta=1$  initially centered at the origin  $X_0=0$ , is considered. The dependence of the PW-induced soliton mean transverse velocity  $\langle \kappa \rangle$  on the PW parameters, namely, its amplitude ( $\alpha$ ), spatial amplitude period ( $T$ ), duty cycle ( $dc$ ), and velocity ( $k$ ) is studied.

The PW can be affected due to the presence of a soliton through the mechanism of the modulational instability (MI). Each one of the discrete spectral components of the PW is associated with a finite bandwidth where the MI can take place. If the spectral content of the soliton falls into these areas and, at the same time, leads to a considerable growth

rate, then the PW is significantly distorted. This can actually be avoided by restricting the amplitude of the PW to small values [15,22]. The spectral range, where each spectral component ( $k_n$ ) of the PW undergoes MI, is centered around  $k_n$  and its width is  $\Delta k = 2a_n^2$ . On the other hand, the spectral content of the soliton [with a zero initial ( $Z=0$ ) transverse velocity, as it will be considered in the following] is centered around the origin with a width that is inversely proportional to its temporal width ( $1/n$ ). Thus, it is possible to prevent MI and the associated PW deformation by appropriately choosing the PW velocity (which results in a shift in all  $k_n$ s), the soliton width, and the PW amplitude. Moreover, even for the case where a spectral component of the soliton falls into the wave number range of the MI, the corresponding growth rate has a finite value, so that the effect of MI can still be small rendering the laminar propagation distance suitable for potential applications in optical devices.

In the following, small amplitude PWs are considered. This is a basic requirement for the application of the perturbation method and, furthermore, ensures a very limited PW deformation due to the superposition of one or two solitons; the initial conditions ( $Z=0$ ) which are fed into the full numerical simulations of the original NLS equation consist of a PW superimposed on one or two such solitons. It will be shown that the results thus obtained are in fact in good agreement with the perturbation method which is based on the assumption of a fixed (unaffected) PW.

Figure 2 depicts soliton propagation for the cases of a PW having  $\alpha=0.1$ ,  $T=4$ ,  $dc=0.5$ , and  $k=1(a,c,e), 2(b,d,f)$ . It is evident that results obtained via direct numerical integration of the NLS Eq. (1) are in good agreement with the results provided by the perturbation analysis, with respect to both soliton displacement as well as soliton amplitude oscillations. The latter are compared in Figs. 2(e) and 2(f), where the fast amplitude oscillations shown in results obtained with direct numerical integration are due to the fact that the dynamically evolving PW is superimposed to the soliton amplitude.

The mean soliton velocity  $\langle \kappa \rangle$  is expected to depend strongly on the initial soliton position with respect to the PW. As shown in Fig. 3(a), depending on  $X_0$ , soliton can have positive or negative transverse velocity. The dependency on  $X_0$  is symmetric with respect to the origin (due to the symmetry of the PW) and it is periodic with a period that differs from the PW amplitude period  $T$  due to the nonzero PW transverse velocity. In comparison with purely sinusoidal PW [14], this dependence on  $X_0$  is more complex, with more local extrema within a period. Moreover, these extrema are not symmetric with respect to zero, meaning that the specific PW parameter selection renders one direction more preferable than the other. The duty cycle ( $dc$ ) of the PW is also shown to determine both the amplitude and the sign of soliton mean transverse velocity  $\langle \kappa \rangle$  as illustrated in Fig. 3(b). The limiting cases  $dc=0$  and  $dc=1$  correspond to purely sinusoidal PW of opposite sign and the results are in accordance with Ref. [14]. The PW transverse velocity ( $k$ ) is also crucial for the soliton velocity  $\langle \kappa \rangle$ , as shown in Fig. 3(c). The corresponding curve is antisymmetric with respect to the origin, meaning that opposite PW velocities induce opposite

soliton velocities. This result is in agreement with the case of a sinusoidal PW in both one-dimensional [14] and two-dimensional [15] media. However, unlike these cases where it was shown that the single maximum soliton velocity is achieved for  $k \approx \eta^{-1}$ , in our case several local extrema are present due to the more complicated form of the PW. The sign of soliton velocity can be different even for two PW velocities with the same sign. Finally, the effect of the spatial period of the amplitude of the PW on the soliton velocity is depicted in Fig. 3(d). In all cases, it is shown that controllable soliton steering can take place by varying a specific PW parameter while keeping the rest constant. Moreover, the quasiparticle perturbation method and the resulting dynamical system [Eqs. (8)–(11)] are shown capable of providing accurate results as compared with results from the numerical integration of the original model (1).

### III. TWO-SOLITON INTERACTIONS

In the following we consider the effect of a PW on the interactions between two initially well-separated solitons. In order to apply the quasiparticle perturbation method, we consider the superposition

$$u = u_s^{(1)} + u_s^{(2)} + u_{pw}, \quad (12)$$

where  $u_s^{(i)}$ ,  $i=1,2$  and  $u_{pw}$  are given by Eqs. (2) and (3), respectively. By substituting Eq. (12) in Eq. (1) and separating terms on the basis of the degree of overlapping, as in the case where only mutual soliton interactions (with no PW) are studied [20], the following equations are obtained:

$$i \frac{\partial u_s^{(i)}}{\partial Z} + \frac{1}{2} \frac{\partial^2 u_s^{(i)}}{\partial X^2} + |u_s^{(i)}|^2 u_s^{(i)} = R^{(i)}(u_s^{(i)}, u_s^{(3-i)}, u_{pw}), \quad i=1,2, \quad (13)$$

where

$$R^{(i)}(u_s^{(i)}, u_s^{(3-i)}, u_{pw}) = - [(u_s^{(i)})^2 (u_s^{(3-i)})^* + 2|u_s^{(i)}|^2 u_s^{(3-i)}] + R^{(i)}(u_s^{(i)}, u_{pw}), \quad (14)$$

with  $R^{(i)}(u_s^{(i)}, u_{pw})$  defined as in Eq. (7). These equations govern soliton evolution, as modified due to their mutual interaction as well as the presence of the PW. The application of the standard perturbation method in Eq. (13) results in the following dynamical system, governing the evolution of soliton parameters under propagation:

$$\begin{aligned} \frac{d\eta^{(i)}}{dZ} &= (-1)^{i+1} 4U_{tot}^3 e^{-U_{tot}\Delta X} \sin(\Delta\phi) \\ &+ \frac{\pi(\eta^{(i)})^2}{2} \sum_{n=-\infty}^{+\infty} a_n \operatorname{sech}\left(\frac{\omega_n^{(i)}\pi}{2}\right) [(\omega_n^{(i)})^2 + 1] \sin(A_n^{(i)}), \end{aligned} \quad (15)$$

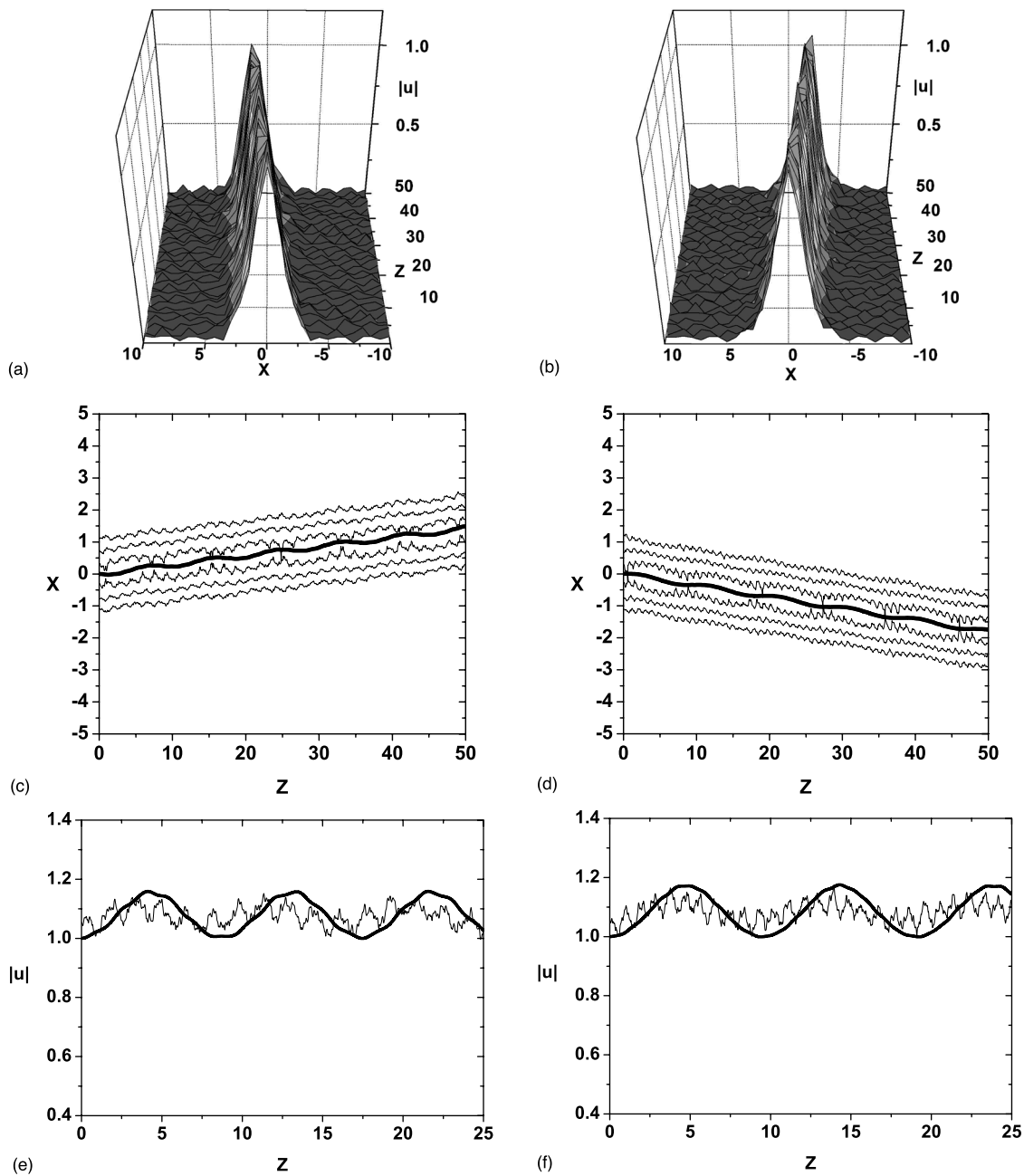


FIG. 2. Soliton displacement (steering) and amplitude oscillations under interaction with a PW of rectangular profile. [(a) and (b)] are the respective 3D plots of [(c) and (d)]. A thick line depicts results from the perturbation method;  $\alpha=0.1$ ,  $T=4$ ,  $dc=0.5$ , and [(a), (c), (e)]  $k=1$ , [(b), (d), (f)]  $k=2$ .

$$\begin{aligned} \frac{d\kappa^{(i)}}{dZ} &= (-1)^{i+1} 4U_{tot}^3 e^{-U_{tot}\Delta X} \cos(\Delta\phi) \\ &- \frac{\pi(\eta^{(i)})^2}{2} \sum_{n=-\infty}^{+\infty} a_n \omega_n^{(i)} \operatorname{sech}\left(\frac{\omega_n^{(i)}\pi}{2}\right) [(\omega_n^{(i)})^2 \\ &+ 1] \sin(A_n^{(i)}), \end{aligned} \quad (16)$$

$$\begin{aligned} \frac{dX_0^{(i)}}{dZ} &= -\kappa^{(i)} - 2U_{tot} e^{-U_{tot}\Delta X} \sin(\Delta\phi) \\ &- \frac{\pi}{2} \sum_{n=-\infty}^{+\infty} a_n \operatorname{sech}\left(\frac{\omega_n^{(i)}\pi}{2}\right) \\ &\times \left\{ -\frac{\pi}{2} \tanh\left(\frac{\omega_n^{(i)}\pi}{2}\right) [(\omega_n^{(i)})^2 + 1] + 2\omega_n^{(i)} \right\} \\ &\times \cos(A_n^{(i)}) \end{aligned} \quad (17)$$

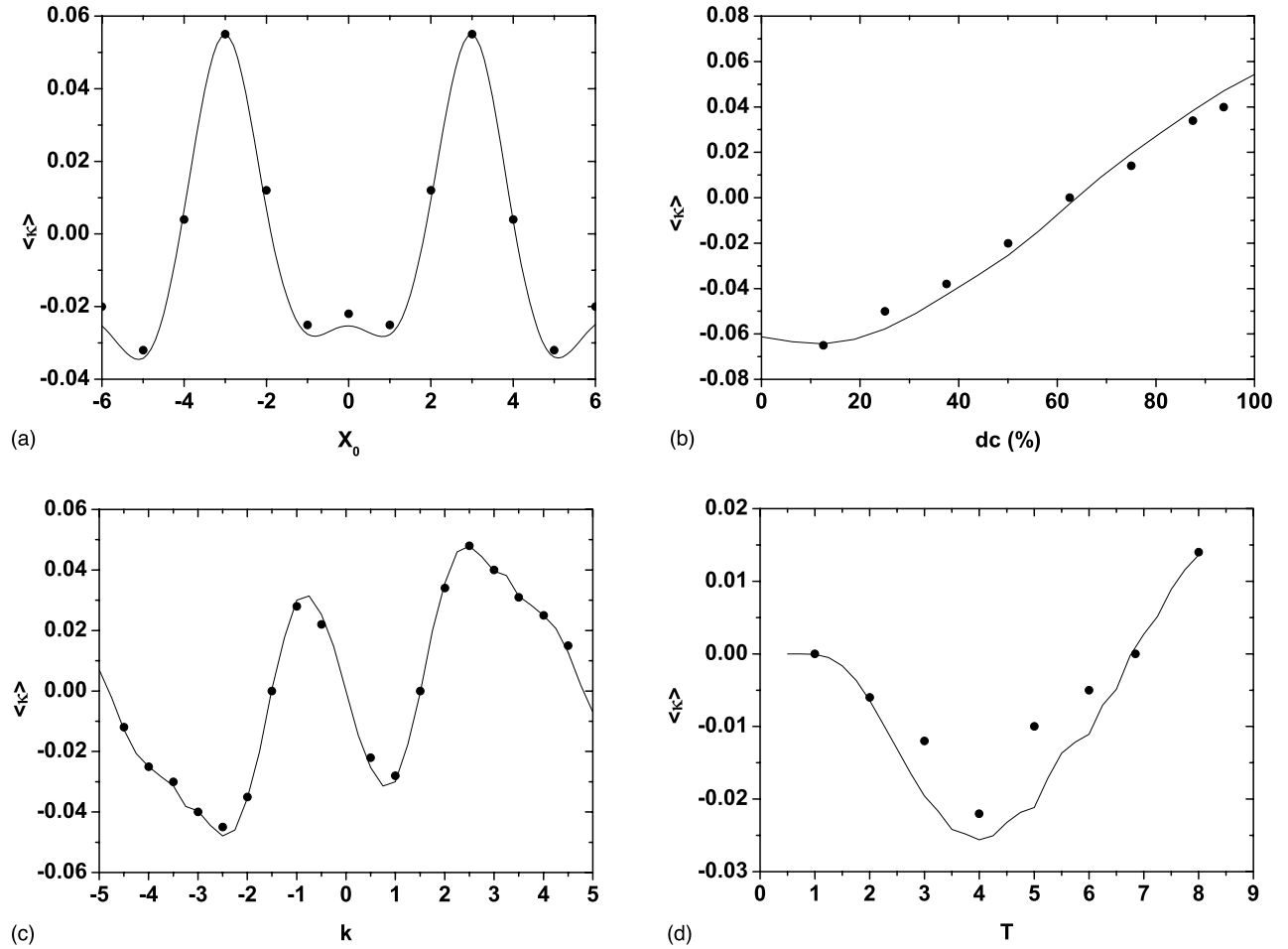


FIG. 3. Soliton mean transverse velocity ( $\langle \kappa \rangle$ ) dependence on the PW parameters. A solid line depicts results from the perturbation method while black dots represent results from direct simulations:  $\alpha=0.1$ ,  $T=4$ ,  $dc=0.5$ , and  $k=0.5$ . Dependence is on (a)  $X_0$ , (b)  $dc$ , (c)  $k$ , (d)  $T$ .

$$\begin{aligned}
 \frac{d\delta^{(i)}}{dZ} &= \frac{1}{2}[(\eta^{(i)})^2 - (\kappa^{(i)})^2] + X_0^{(i)} \frac{d\kappa^{(i)}}{dZ} \\
 &- 2U_{tot} K_{tot} e^{-U_{tot}\Delta X} \sin(\Delta\phi) + 6U_{tot}^2 e^{-U_{tot}\Delta X} \cos(\Delta\phi) \\
 &+ \frac{\pi\eta^{(i)}}{2} \sum_{n=-\infty}^{+\infty} a_n \operatorname{sech}\left(\frac{\omega_n^{(i)}\pi}{2}\right) \left\{ \frac{\omega_n^{(i)}\pi}{2} \tanh\left(\frac{\omega_n^{(i)}\pi}{2}\right) \right. \\
 &\left. \times [(\omega_n^{(i)})^2 + 1] + 2 \right\} \cos(A_n^{(i)}), \quad (18)
 \end{aligned}$$

where  $\omega_n^{(i)} = (k_n - \kappa^{(i)})/\eta^{(i)}$ ,  $A_n^{(i)} = (k_n - \kappa^{(i)})X_0^{(i)} + (1/2)k_n^2 Z + \kappa^{(i)}X_0^{(i)} + \delta^{(i)} - \phi_n$ ,  $\Delta\phi = K_{tot}\Delta X + \delta^{(1)} - \delta^{(2)}$ ,  $\delta^{(i)} = \sigma^{(i)} - \kappa^{(i)}X_0^{(i)}$ ,  $\Delta X = X_0^{(1)} - X_0^{(2)}$ ,  $U_{tot} = (\eta^{(1)} + \eta^{(2)})/2$ ,  $K_{tot} = (\kappa^{(1)} + \kappa^{(2)})/2$ .

In the following, we are focusing on the cases where the interaction between two solitons can be qualitatively altered due to the presence of a PW. Conditions under which a strong soliton interaction can be either prevented or provoked because of the presence of the PW are investigated. For the case of zero PW transverse velocity  $k=0$ , the PW does not lead to a qualitative differentiation of soliton inter-

actions: When two solitons do not interact with each other, the PW simply results in amplitude oscillations of the solitons. When the solitons collide for a zero PW, they still collide, but in a different propagation distance, under the presence of a PW. However, the case of a PW having nonzero velocity  $k \neq 0$  is shown to have a much more drastic effect on soliton interactions.

The case of propagation of two solitons initially located at  $X_0^{(1),(2)} = 3.5, -3.5$  is shown in Fig. 4(a) where there is no PW and the mutual soliton interaction result in attraction and elastic collision. The presence of a PW, having  $\alpha=0.05$ ,  $T=15$ ,  $dc=0.5$ , and  $k=0.5$ , is shown capable of reducing mutual soliton attraction and completely preventing collision as illustrated in Figs. 4(b) and 4(c). However, the effect of the PW depends strongly on its parameters, that is, for some parameter choices the collision is not prevented [Figs. 4(d) and 4(e)] or the two solitons just “touch” and separate [Figs. 4(f) and 4(g)]. For the cases where the two solitons collide or approach very close, the results of the perturbation method deviate significantly from direct numerical simulations [Figs. 4(d) and 4(f)]. This is because the separation of the nonlinear term on the basis of the degree of overlapping and the cor-

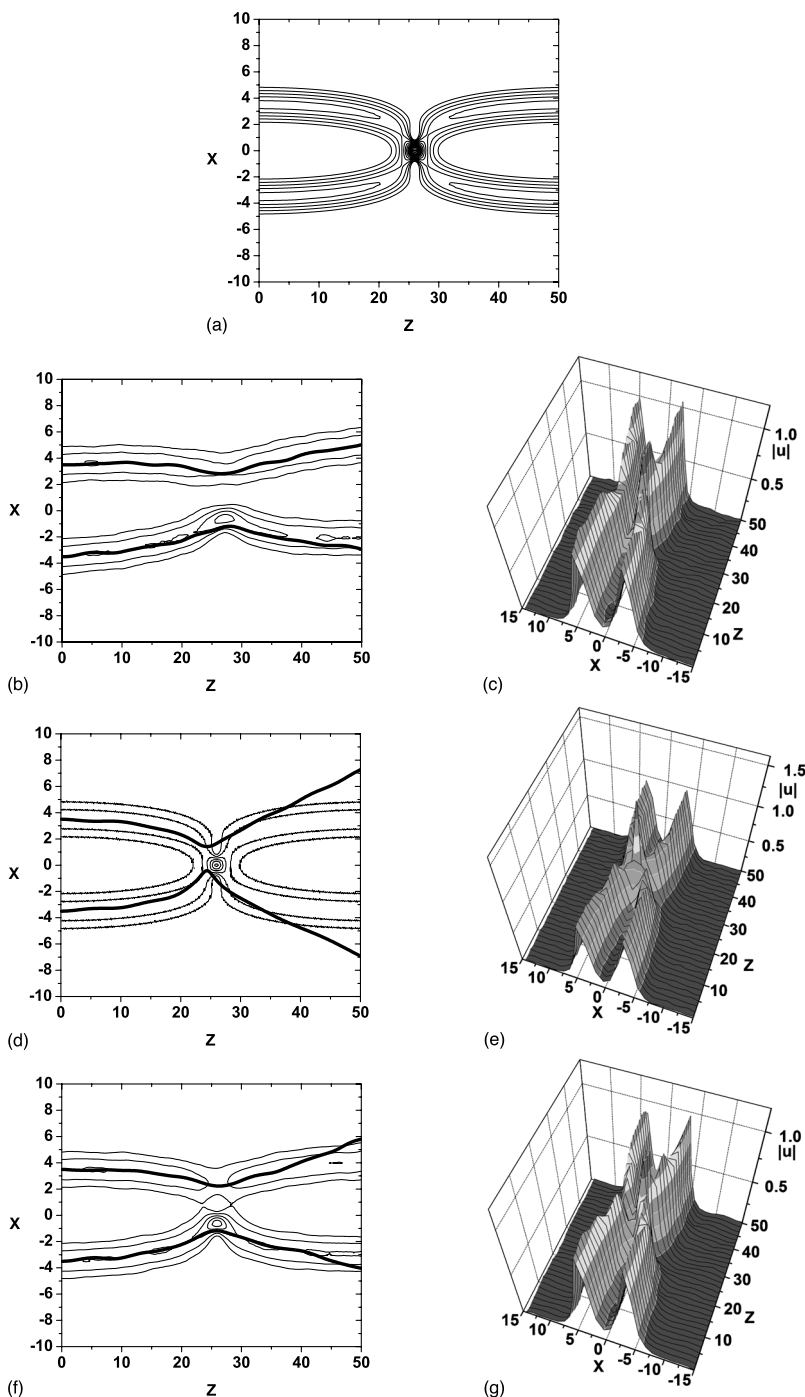


FIG. 4. Two-soliton interaction ( $X_0^{(1),(2)}=3.5, -3.5$ ) under the presence of a PW having  $\alpha=0.05$ ,  $dc=0.5$ , and  $k=0.5$ . (c), (e) and (g) are the respective 3D plots of (b), (d) and (f). A thick line depicts results from the perturbation method. (a) No PW is induced. [(b) and (c)]  $T=15$  complete collision avoidance. [(d) and (e)]  $T=1$  collision is not prevented. [(f) and (g)]  $T=20$  close approach.

responding Eq. (13) become meaningless. However, it is remarkable that, even in these cases the collision distance is well predicted by the perturbation method.

Apart from preventing soliton collision, the presence of a PW can also enhance mutual soliton interaction in a symmetric or asymmetric way. As shown in Figs. 5(a)–5(i), a PW, with  $\alpha=0.1$ ,  $T=4$ ,  $dc=0.5$ , and  $k=0.5$ , can cause symmetric [Figs. 5(b) and 5(c)] or asymmetric [Figs. 5(e) and 5(f) and Figs. 5(h) and 5(i)] attraction between the two solitons, depending strongly on the relative initial soliton positions, with respect to the PW.

#### IV. SUMMARY AND CONCLUSIONS

In conclusion, spatial soliton dynamics in optically induced photonic lattices have been studied. The PW induced potential is shown capable of drastically affecting the evolution of parameters of the initial beams, such as the transverse velocity and the amplitude. On the other hand, soliton mutual interaction can either be increased or reduced by appropriately selecting the PW-induced photonic lattice features such as the period, the amplitude, the relative position with respect to the soliton beam center, and the pulse duration in case of rectangular PW lattice. The quasiparticle perturbation

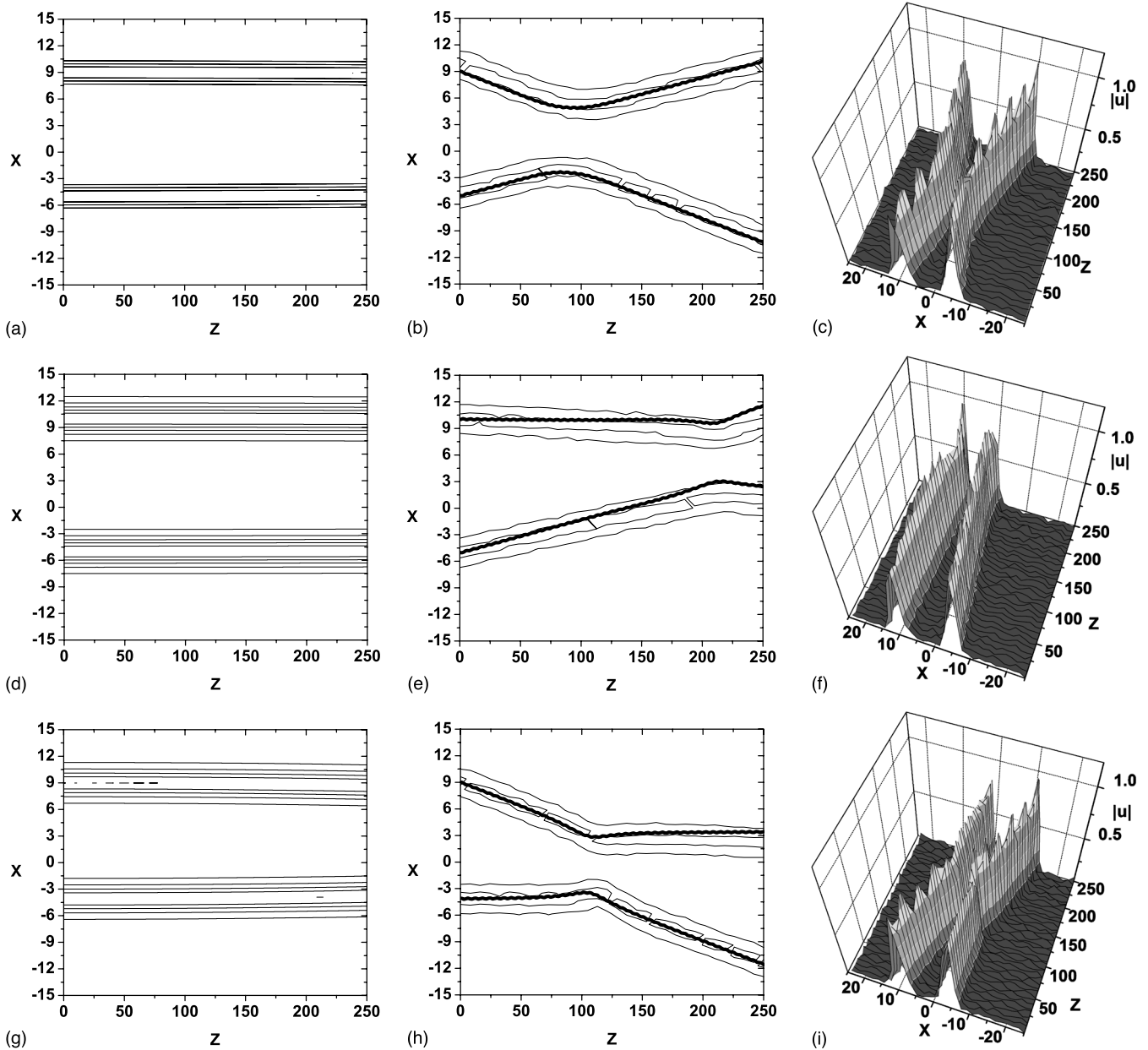


FIG. 5. Two-soliton mutual interaction enhancement under the presence of a PW having  $\alpha=0.1$ ,  $T=4$ ,  $dc=0.5$ , and  $k=0.5$ . [(c), (f), (i)] are the respective 3D plots of [(b), (e), (h)]. A thick line depicts results from the perturbation method. Symmetric attraction case for  $X_0^{(1),(2)}=9.0, -5.0$  (a) no PW and [(b) and (c)] PW present. Asymmetric attraction case for  $X_0^{(1),(2)}=10.0, -5.0$  (d) no PW and [(e) and (f)] PW present. Asymmetric attraction case  $X_0^{(1),(2)}=9.0, -4.1$  (g) no PW and [(h) and (i)] PW present.

approach is shown to provide an accurate description of soliton evolution under the presence of a PW in the case of a single soliton as well as in the case of two-soliton interactions. The results of the perturbation method apply to any kind of linear PW, thus providing a useful tool for efficient PW design and parameter selection in order to achieve the desirable soliton evolution, in terms of dynamically reconfig-

urable all-optical control.

**ACKNOWLEDGMENTS**

This project is co-funded by the European Social Fund (75%) and National Resources (25%)-Operational Program for Educational and Vocational Training II (EPEAEK II), and particularly the Program PYTHAGORAS.

- [1] A. A. Sukhorukov, Y. S. Kivshar, H. S. Eisenberg, and Y. Silberberg, *IEEE J. Quantum Electron.* **39**, 31 (2003).
- [2] J. W. Fleischer, G. Bartal, O. Cohen, T. Schwartz, O. Manela, B. Freedman, M. Segev, H. Buljan, and N. K. Efremidis, *Opt. Express* **13**, 1780 (2005).
- [3] A. A. Sukhorukov and Y. S. Kivshar, *Phys. Rev. Lett.* **87**, 083901 (2001).
- [4] D. Mandelik, R. Morandotti, J. S. Aitchison, and Y. Silberberg, *Phys. Rev. Lett.* **92**, 093904 (2004).
- [5] W. Krolikowski and Y. S. Kivshar, *J. Opt. Soc. Am. B* **13**, 876 (1996).
- [6] R. Y. Chiao, *Spatial Solitons*, in *Springer Series in Optical Sciences*, edited by S. Trillo and W. Torruellas, (Springer-Verlag, Berlin, 2001).
- [7] Y. S. Kivshar and G. P. Agrawal, *Optical Solitons-From Fibers to Photonic Crystals*, edited by Yuri S. Kivshar and Govind Agrawal (Academic Press, California, 2003).
- [8] N. K. Efremidis, S. Sears, D. N. Christodoulides, J. W. Fleischer, and M. Segev, *Phys. Rev. E* **66**, 046602 (2002).
- [9] D. Neshev, E. Ostrovskaya, Y. Kivshar, and W. Krolikowski, *Opt. Lett.* **28**, 710 (2003).
- [10] J. W. Fleischer, T. Carmon, M. Segev, N. K. Efremidis, and D. N. Christodoulides, *Phys. Rev. Lett.* **90**, 023902 (2003).
- [11] Z. Chen, H. Martin, E. D. Eugenieva, and J. Xu, *Opt. Express* **13**, 1816 (2005).
- [12] M. J. Ablowitz, K. Julien, Z. H. Musslimani, and M. I. Weinstein, *Phys. Rev. E* **71**, 055602(R) (2005).
- [13] I. L. Garanovich, A. A. Sukhorukov, and Y. S. Kivshar, *Opt. Express* **13**, 5704 (2005).
- [14] Y. Kominis and K. Hizanidis, *J. Opt. Soc. Am. B* **21**, 562 (2004).
- [15] Y. Kominis and K. Hizanidis, *J. Opt. Soc. Am. B* **22**, 1360 (2005).
- [16] R. Scharf and A. R. Bishop, *Phys. Rev. E* **47**, 1375 (1993).
- [17] Y. V. Kartashov, A. S. Zelenina, L. Torner, and V. A. Vysloukh, *Opt. Lett.* **29**, 766 (2004).
- [18] Y. V. Kartashov, L. Torner, and D. N. Chistodoulides, *Opt. Lett.* **30**, 1378 (2005).
- [19] Y. S. Kivshar and B. Malomed, *Rev. Mod. Phys.* **61**, 763 (1989).
- [20] A. Hasegawa and Y. Kodama, *Solitons in Optical Communications*, Oxford Series on Optical and Imaging Sciences, edited by Akira Hasegawa, M. Lapp, J. Nishizawa, B. B. Snavely, H. Stark, A. C. Tam, and T. Wilson (Clarendon Press, Oxford, 1995).
- [21] Y. Kominis and K. Hizanidis, *Opt. Commun.* **234**, 193 (2004).
- [22] A. B. Aceves, C. De Angelis, and S. Wabnitz, *Opt. Lett.* **17**, 1758 (1992).